frontiers in Chemical Biology

TYPE Original Research
PUBLISHED 04 September 2026
DOI 10.3389/fchbi.2026.1888764

OPEN ACCESS

EDITED BY
Elizabeth Igne Ferreira,
University of São Paulo, Brazil

REVIEWED BY
Ramon Guerra De Oliveira,
Brazilian Biosciences National Laboratory (LNBio), Brazil
Angel Lobo-Rojas,
National Center for Research in Energy and Materials, Brazil

*CORRESPONDENCE
Guillermo R. Labadie,
labadie@iquir-conicet.gov.ar

†PRESENT ADDRESS
Babu L. Tekwani,
GlobaCure, Birmingham, AL, United States

RECEIVED 22 May 2026
REVISED 16 July 2026
ACCEPTED 21 July 2026
PUBLISHED 04 September 2026

CITATION
Recio-Balsells AI, Panozzo-Zenere EA, Coser EM, Ferreira BA, Coelho AC, Wilkinson SR, Tekwani BL and Labadie GR (2026) Second-generation N,N′-disubstituted aliphatic diamines: discovery of potent hits for multi-species leishmaniasis treatment.
Front. Chem. Biol. 5:1888764.
doi: 10.3389/fchbi.2026.1888764

Second-generation N,N′-disubstituted aliphatic diamines: discovery of potent hits for multi-species leishmaniasis treatment

Alejandro I. Recio-Balsells[1], Esteban A. Panozzo-Zenere[1], Elizabeth M. Coser[2], Bianca A. Ferreira[2], Adriano Cappellazzo Coelho[2], Shane R. Wilkinson[3], Babu L. Tekwani[4†] and Guillermo R. Labadie[1,5*]

[1]Instituto de Química Rosario (IQUIR-CONICET-UNR), Universidad Nacional de Rosario, Rosario, Argentina, [2]Departamento de Biologia Animal, Instituto de Biologia, Universidade Estadual de Campinas (UNICAMP), Campinas, Brazil, [3]School of Biological and Chemical Sciences, Queen Mary University of London, London, United Kingdom, [4]National Center for Natural Products Research & Department of Biomolecular Sciences, School of Pharmacy, University of Mississippi, Oxford, MS, United States, [5]Departamento de Química Orgánica, Facultad de Ciencias Bioquímicas y Farmacéuticas, Universidad Nacional de Rosario, Rosario, Argentina

Kinetoplastid diseases remain a major global health challenge, highlighting the need for new antiparasitic chemotypes. *N,N′*-disubstituted aliphatic diamines have emerged as a promising scaffold against trypanosomatid parasites. Building on our previous studies, we expanded the structure–activity relationship (SAR) of this chemotype through the synthesis of fifty-two analogues obtained by one-pot reductive amination of aliphatic diamine linkers with structurally diverse aromatic and heteroaromatic aldehydes. The compounds were first evaluated against the extracellular stages of *Trypanosoma cruzi*, *Trypanosoma brucei*, and *Leishmania donovani*. Several derivatives displayed pIC_{50} values above 6.0 and Vero-cell selectivity index above 10. Based on these results, nine hits were further evaluated against the promastigote and amastigote stages of *L. amazonensis*, *L. braziliensis*, and *L. infantum,* responsible for cutaneous and visceral leishmaniasis. Among them, compounds 12a, 12m, and 8e showed potent activity against intracellular amastigotes with selectivity indices above 10, highlighting this scaffold as a promising starting point for antileishmanial drug discovery.

KEYWORDS
antileishmanials, broad-spectrum, *Leishmania* spp., polyamines, trypanosomatids

1 Introduction

Diseases caused by protozoa of the family Trypanosomatidae remain a major global health challenge, particularly in tropical and subtropical regions where structural inequalities amplify their impact (World Health Organization WHO, 2021). Human African trypanosomiasis (HAT), Chagas disease, and leishmaniasis are caused by *Trypanosoma brucei gambiense* or *T. b. rhodesiense*, *T. cruzi*, and several *Leishmania* species, respectively. Although progress in surveillance and vector control has reduced the incidence of HAT, the burden of chronic Chagas disease and visceral leishmaniasis

remains high. According to World Health Organization (WHO) estimates, approximately 700,000 to 1 million new cases of leishmaniasis occur annually (World Health Organization, 2026a), around 8 million people are infected with *T. cruzi* (World Health Organization, 2026b), and fewer than 1,000 new cases of HAT are reported each year (World Health Organization, 2026c).

Available treatments are limited by toxicity, prolonged administration, stage-specific efficacy, and emergence of drug resistance. In particular, therapeutic options for chronic Chagas disease and leishmaniasis remain suboptimal, highlighting the need for new molecular entities acting through validated and parasite-selective mechanisms (Pathak et al., 2023; Olías-Molero et al., 2021). The DNDi (2026), a non-profit research organization, has had a major impact on the development of therapies for neglected tropical diseases, including those caused by trypanosomatid parasites. This example highlights the importance of collaborative initiatives in advancing anti-trypanosomatid drug discovery, particularly for diseases that require substantial investment in late-stage clinical development (Ma et al., 2023). Regarding leishmaniasis, DNDi, in collaboration with other partners, has developed several promising small-molecule leads that have advanced to clinical stages, including LXE408 (Nagle et al., 2020), DNDI-6148 (Mowbray et al., 2021), DNDI-6899 (Thomas et al., 2019) and DNDI-6174 (Braillard et al., 2023). In contrast, the drug pipeline for Chagas disease has remained constrained. Nevertheless, the oxaborole scaffold is emerging as a promising source of clinical candidates, with the benzoxaborole DNDI-6148, initially developed for leishmaniasis, also demonstrating promising activity against *T. cruzi* (DNDi, 2026).

Leishmaniasis comprises a spectrum of diseases caused by several *Leishmania* species and manifests in three main clinical forms: cutaneous leishmaniasis, characterized by skin lesions; mucocutaneous leishmaniasis, affecting the mucosa of the nose, mouth, and throat; and visceral leishmaniasis, the most severe form, which affects the spleen, liver, and bone marrow and is fatal if left untreated. These manifestations are mainly associated with the infecting *Leishmania* species. For example, visceral leishmaniasis is primarily caused by *L. donovani* and *L. infantum*, whereas cutaneous and mucocutaneous forms are typically associated with species such as *L. major*, *L. tropica*, *L. braziliensis*, *L. mexicana*, and *L. amazonensis* (Selvapandiyan et al., 2025). These species also display distinct geographical distributions: *L. major*, *L. tropica*, and *L. donovani* are prevalent in Africa and Eurasia, while *L. mexicana*, *L. amazonensis*, and *L. braziliensis* are endemic in the Americas. In this context, target product profiles (TPPs) play a crucial role in guiding antiparasitic drug discovery efforts, emphasizing the importance of identifying lead molecules with activity against a broad spectrum of *Leishmania* species (DNDi, 2026; Rao et al., 2019).

Chemical biology approaches to drug discovery seek to exploit mechanistic vulnerabilities in pathogen metabolism through the rational design of small molecules capable of perturbing essential biological pathways. In trypanosomatids, polyamine homeostasis represents one such vulnerability, as polyamines play critical roles in DNA stabilization, translation, stress adaptation, and cell proliferation (Phillips, 2018). Importantly, spermidine is required for the biosynthesis of trypanothione, a unique dithiol that replaces glutathione as the major intracellular thiol in trypanosomatids (Fairlamb et al., 1985). This trypanothione-dependent redox network is absent in mammalian cells, creating a distinctive pathogen-selective biochemical node that can be selectively targeted. Moreover, the clinical success of eflornithine, an inhibitor of ornithine decarboxylase, validates polyamine metabolism as a tractable therapeutic target against trypanosomatids (Bacchi et al., 1980). Furthermore, several polyamine-based drug discovery programs have yielded compounds with antileishmanial activity including, 3-aminooxy-1-aminopropane (APA) (Singh et al., 2007), γ-guanidinooxypropylamine (GAPA) (Singh et al., 2008), spermine analogs (Mukhopadhyay and Madhubala, 1995), *N*-arylspermidines (Mollo et al., 2025) and pyridine heterocyclic diamines (Martín-Montes et al., 2021), among others (Figure 1).

Collectively, these studies demonstrate that structurally diverse diamine-based scaffolds constitute a promising source of antitrypanosomatid agents and provide a rationale for the development of simplified synthetic analogues with improved drug-like properties. Inspired by this biological framework, we previously developed a library of *N*,*N*′-disubstituted aliphatic diamines designed as simplified and synthetically accessible polyamine-inspired scaffolds. Several compounds exhibited pIC_{50} values above 6.0 and SI values above 10 against the extracellular stages of *T. cruzi*, *T. brucei*, and *L. donovani* (Caminos et al., 2012). In subsequent studies, several diamines also exhibited potent activity against the clinically relevant intracellular amastigote stage of *T. cruzi* (Recio-Balsells et al., 2026). Furthermore, we reported the expanded synthesis of second-generation analogues and also characterized their activity against apicomplexan parasites (Recio-Balsells et al., 2025). These compounds exhibited submicromolar activity against resistant strains of *Plasmodium falciparum*. These findings established this scaffold as a valuable starting point for antiparasitic drug discovery.

Building on these findings, the aim of the present study was to define the antitrypanosomatid structure–activity relationships of this second-generation diamine library and to identify lead compounds for expanded evaluation against clinically relevant *Leishmania* species.

Accordingly, we evaluated the fifty-two second-generation *N*,*N*′-disubstituted diamines against the extracellular stages of *T. cruzi*, *T. brucei*, and *L. donovani*. Based on their antiparasitic activity, selectivity indices, and chemical diversity, nine analogues were advanced for further evaluation against the promastigote and amastigote stages of additional *Leishmania* species, including *L. amazonensis*, *L. braziliensis*, and *L. infantum* responsible for cutaneous and visceral leishmaniasis.

2 Results and discussion

2.1 Chemistry

We previously reported the synthesis of a library of thirty *N*,*N*′-disubstituted aliphatic diamines that demonstrated significant activity against trypanosomatid parasites (Supplementary Table S2, Supplementary Material) (Caminos et al., 2012). The synthetic strategy, based on a one-pot reductive amination between 1,ω-aliphatic diamines and substituted aromatic

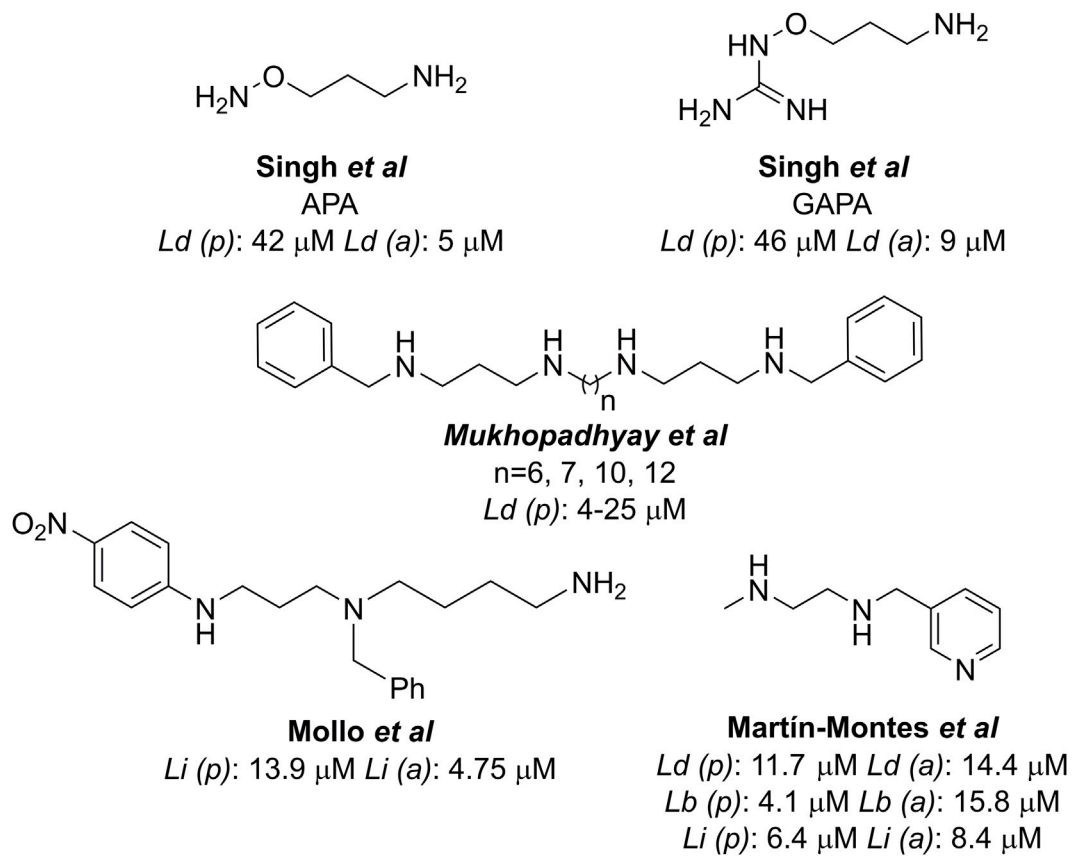

FIGURE 1
Polyamine-based compounds active against *Leishmania spp*. Legend: *Ld: L. donovani, Lb: L. Braziliensis, Li: L. Infantum, (p):* promastigote, *(a)*: amastigote.

aldehydes, was described in detail in our earlier work and is therefore not reiterated here. Briefly, the parent collection incorporated aliphatic diamine chain lengths ranging from three to twelve carbon atoms (n = 3, 4, 6, 8, 10, 12) and benzaldehyde derivatives bearing oxygenated substituents such as methoxy and benzyloxy groups.

To further expand the chemical space within this scaffold, we introduced a new panel of aromatic and heteroaromatic aldehydes designed to systematically evaluate steric, electronic, and lipophilic effects (Scheme 1) (Recio-Balsells et al., 2025). A 4-isopropyl substituent was selected to evaluate the impact of increased hydrophobicity relative to the previously explored oxygenated derivatives. In contrast, 4-nitrobenzaldehyde was incorporated to assess the influence of a strong electron-withdrawing group and potential mechanistic parallels with nitro-containing antiparasitic agents such as nifurtimox, benznidazole, and fexinidazole, whose bioactivation in trypanosomatids involves type I nitroreductases absent in mammalian hosts (Wyllie et al., 2016).

Bulky aromatic systems, including 2-naphthyl and biphenyl aldehydes, were introduced to investigate the effect of extended π-surfaces and increased steric demand. Given the favorable activity observed for oxygenated derivatives in the initial series, 3,4-dibenzyloxybenzaldehyde was selected to evaluate the tolerance for more sterically demanding oxygen-containing substituents. Moreover, heteroaromatic aldehydes (furan-2-carboxaldehyde and pyrrole-2-carboxaldehyde) were incorporated to modulate polarity and electronic distribution while maintaining aromatic character. Finally, to further investigate the influence of aromatic substitution within the most promising long-chain analogues, a focused series of twelve derivatives was synthesized from para-halogenated (4-F, 4-Cl, and 4-Br) and para-methyl-substituted benzaldehydes using aliphatic 1,ω-diamines containing 8-, 10-, and 12-carbon linkers. This design was based on the favorable antitrypanosomatid activity previously observed for the structurally simple analogues 10a and 12a, which identified long-chain diamines as a promising platform for further structural diversification.

2.2 Biology

2.2.1 Activities against extracellular stages of *T. cruzi, L. donovani* and *T. brucei*

The collection of fifty-two *N,N′*-bis-benzyl aliphatic diamines (compounds 3f-3l, 4f-4l, 6f-6l, 8f-8p, 10f-10p and 12f-12p) was tested *in vitro* against trypanosomatids (*T. brucei brucei* bloodstream form [trypomastigotes], *T. cruzi* epimastigotes and *L. donovani* promastigotes). To assess mammalian cytotoxicity, Vero cell counterscreens were used as a first-pass assay for the complete library, whereas BMDM counterscreens were reserved for prioritized hit compounds. Vero cell data were previously reported,

10.3389/fchbi.2026.1888764

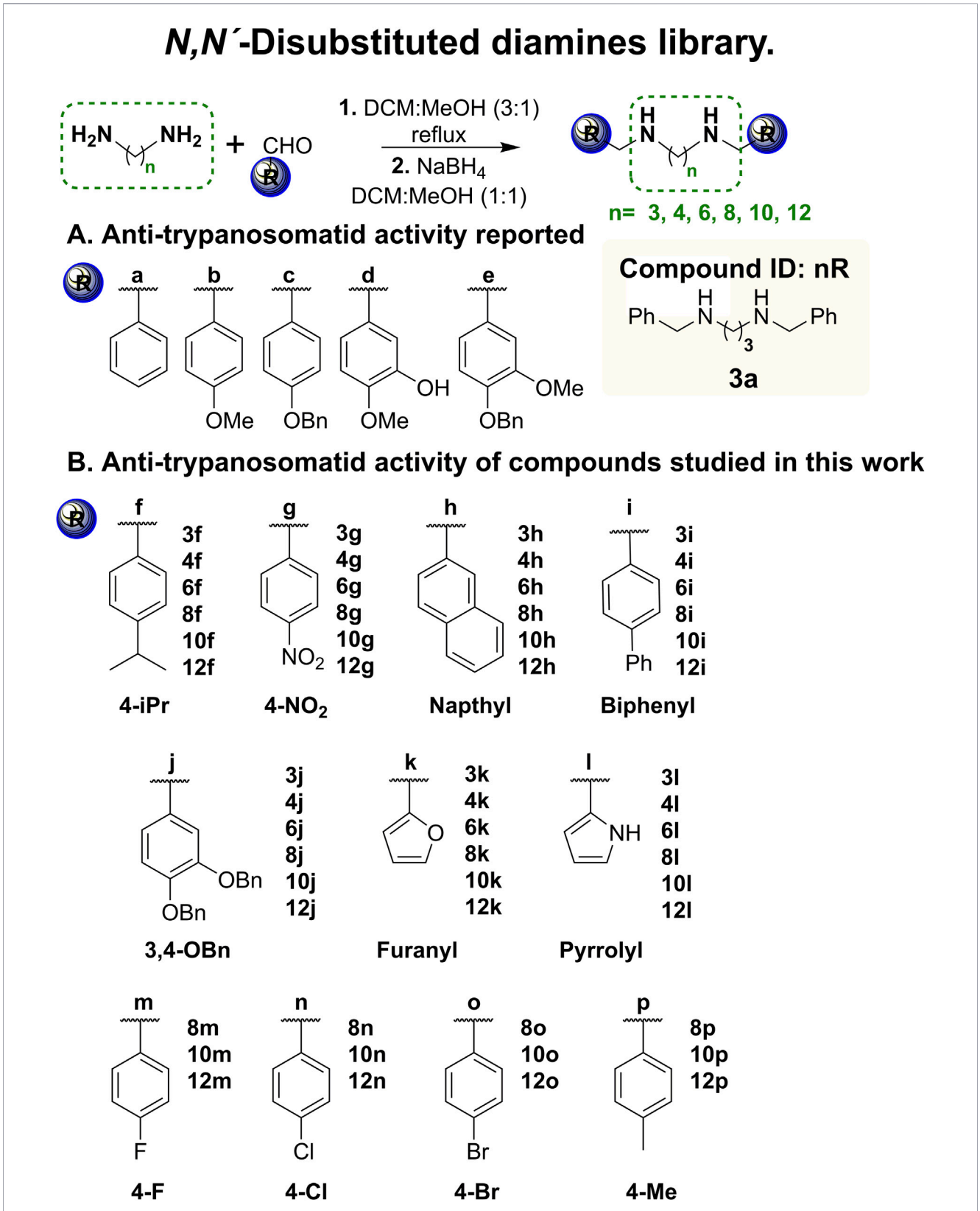

SCHEME 1
N,N′-disubstituted aliphatic diamines studied in this work.

10.3389/fchbi.2026.1888764

TABLE 1 **Antiparasitic activity of *N,N′*-disubstituted diamines.**

ID	n	R	*Ld (p)*[a] pIC_{50}	Selectivity[e] *Ld*/Ctt	*Tc (e)*[b] pIC_{50}	Selectivity[e] *Tc*/Ctt	*Tb*[c] pIC_{50}	Selectivity[e] *Tb*/Ctt	Ctt[d] pIC_{50}
3f	3	4-Isopropyl	6.25	>25.1	6.28	>26.6	6.72	>74.2	<4.85
4f	4	4-Isopropyl	6.17	18.7	6.43	34.3	7.54	437	4.90
6f	6	4-Isopropyl	5.58	2.63	6.41	15.4	7.54	200	5.22
8f	8	4-Isopropyl	6.31	13.5	6.49	20.6	6.85	47.1	5.18
10f	10	4-Isopropyl	5.69	>5.28	6.19	>16.8	6.70	>54.5	<4.96
12f	12	4-Isopropyl	5.24	>1.76	SP	-	SP	-	<4.99
3g	3	4-Nitro	4.70	>0.69	5.09	>1.68	<4.50	-	<4.86
4g	4	4-Nitro	5.13	>1.81	5.19	>2.08	5.07	>1.54	<4.88
6g	6	4-Nitro	5.24	>2.13	5.66	>5.64	5.21	>1.98	<4.91
8g	8	4-Nitro	5.40	>2.90	5.75	>6.50	5.70	>5.72	<4.94
10g	10	4-Nitro	5.68	>5.11	5.71	>5.51	6.13	>14.5	<4.97
12g	12	4-Nitro	4.82	>0.66	SP	-	SP	-	<5.00
3h	3	2-Naphtyl	5.60	>5.40	6.19	>21.1	6.80	>84.4	<4.87
4h	4	2-Naphtyl	5.89	>10.0	6.21	>20.8	7.22	>226	<4.89
6h	6	2-Naphtyl	5.69	>5.89	6.33	>25.5	7.30	>266	<4.92
10h	10	2-Naphtyl	<4.50	-	SP	-	SP	-	<4.98
12h	12	2-Naphtyl	5.44	>2.75	SP	-	SP	-	<5.00
3i	3	4-Biphenyl	6.82	43.8	6.43	17.5	7.96	591	5.19
4i	4	4-Biphenyl	6.23	>19.0	SP	-	SP	-	<4.95
6i	6	4-Biphenyl	5.99	>10.4	SP	-	SP	-	<4.97
8i	8	4-Biphenyl	5.42	>2.61	SP	-	SP	-	<5.00
10i	10	4-Biphenyl	5.33	>2.00	SP	-	SP	-	<5.03
12i	12	4-Biphenyl	4.71	>0.45	SP	-	SP	-	<5.05
3j	3	3.4-diOBn	5.68	>3.32	6.12	>9.39	6.62	>28.8	<5.15
4j	4	3.4-diOBn	5.56	>2.51	SP	-	SP	-	<5.16
6j	6	3.4-diOBn	5.67	>3.09	4.73	>0.35	6.24	>11.4	<5.18
8j	8	3.4-diOBn	5.44	>1.73	6.15	>9.04	6.13	>8.66	<5.19
10j	10	3.4-diOBn	5.08	>0.73	SP	-	SP	-	<5.21
12j	12	3.4-diOBn	4.81	>0.38	SP	-	SP	-	<5.23
3k	3	2-Furanyl	<4.50	>0.18	<4.50	-	<4.50	-	<4.69
4k	4	2-Furanyl	<4.50	>0.17	4.80	>1.20	5.16	>2.75	<4.72
6k	6	2-Furanyl	<4.50	>0.37	5.22	>2.84	5.16	>2.47	<4.76
8k	8	2-Furanyl	4.56	>0.57	5.64	>6.87	5.55	>5.51	<4.81
10k	10	2-Furanyl	4.79	>0.89	5.80	>8.94	5.74	>7.81	<4.84
12k	12	2-Furanyl	5.32	>2.73	5.25	>2.34	6.11	>17.1	<4.88
3L	3	2-Pyrrolyl	<4.50	>0.12	<4.50	-	<4.50	-	<4.69
4L	4	2-Pyrrolyl	<4.50	>0.12	<4.50	-	<4.50	-	<4.71

(*Continued*)

TABLE 1 Continued

ID	n	R	*Ld (p)*[a] pIC_{50}	Selectivity[e] *Ld*/Ctt	*Tc (e)*[b] pIC_{50}	Selectivity[e] *Tc*/Ctt	*Tb*[c] pIC_{50}	Selectivity[e] *Tb*/Ctt	Ctt[d] pIC_{50}
8L	8	2-Pyrrolyl	4.82	>1.03	5.72	>8.18	5.64	>6.88	<4.80
10L	10	2-Pyrrolyl	5.47	>4.29	5.95	>12.7	6.17	>21.4	<4.84
12L	12	2-Pyrrolyl	5.36	>3.02	6.27	>24.6	6.14	>18.4	<4.88
8m	8	4-Fluoro	5.33	>2.80	6.17	>19.7	5.94	>11.6	<4.88
10m	10	4-Fluoro	5.81	>7.97	6.19	>18.9	6.70	>61.5	<4.91
12m	12	4-Fluoro	6.36	>26.5	6.80	>71.3	7.17	>170	<4.94
8n	8	4-Chloro	5.75	5.00	6.23	15.1	6.70	44.5	5.05
10n	10	4-Chloro	5.87	6.69	6.17	13.1	7.17	133	5.05
12n	12	4-Chloro	5.72	>5.94	NT	-	NT	-	<4.95
8o	8	4-Bromo	5.36	>2.27	6.24	>17.3	6.64	>42.9	<5.01
10o	10	4-Bromo	5.43	>2.51	6.00	>9.33	7.11	>120	<5.03
12o	12	4-Bromo	5.95	>7.82	5.82	>5.78	7.10	>111	<5.05
8p	8	4-Methyl	5.62	>5.60	6.32	>28.1	6.62	>56.3	<4.87
10p	10	4-Methyl	5.88	>9.54	6.21	>20.2	7.06	>142	<4.90
12p	12	4-Methyl	5.71	>5.94	5.99	>11.4	7.08	>140	<4.94
		Pentamidine	5.21						
		Amphotericin B	6.49						
		Nifurtimox			5.68		5.77		

[a]*Ld (p)*: *L. donovani* promastigotes pIC_{50} growth inhibition assay tested up to a maximum concentration of 100 μM.
[b]*Tc (e)*: *T. cruzi* epimastigotes pIC_{50} growth inhibition assay tested at maximum concentration of 30 μM.
[c]*Tb*: *T. brucei* trypomastigotes pIC_{50} growth inhibition assay tested up to a maximum concentration of 30 μM.
[d]Ctt: Cytotoxicity was performed against VERO cells up to a maximum concentration of 4.76 μg/mL.
[e]Selectivity index (SI); SI = $IC_{50}^{\text{vero cells}}/IC_{50}^{\text{parasites}}$. NT: Not tested. All drug activity assays were performed in triplicate. SP: Solubility issues, some compounds presented solubility problems as soon as the solution in DMSO was in contact with the corresponding culture medium in activity assays against trypanosomatids (12f and 6-12i).

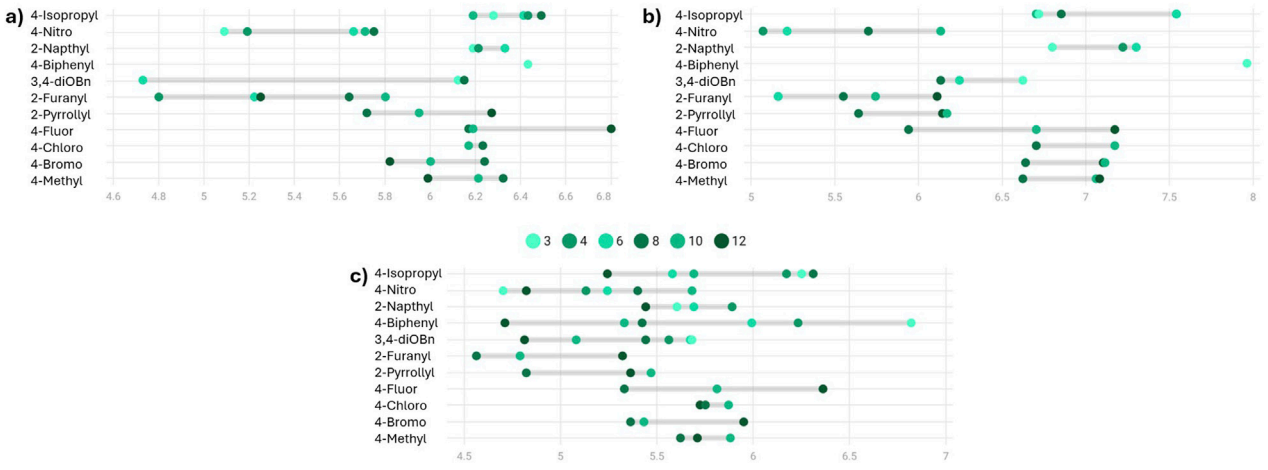

FIGURE 2
Range plot of the anti-trypanosomatid activity (pIC_{50}) for all analogs on *T. cruzi* epimastigotes **(a)**, *T. brucei* trypomastigotes **(b)**, and *L. donovani* promastigotes **(c)**.

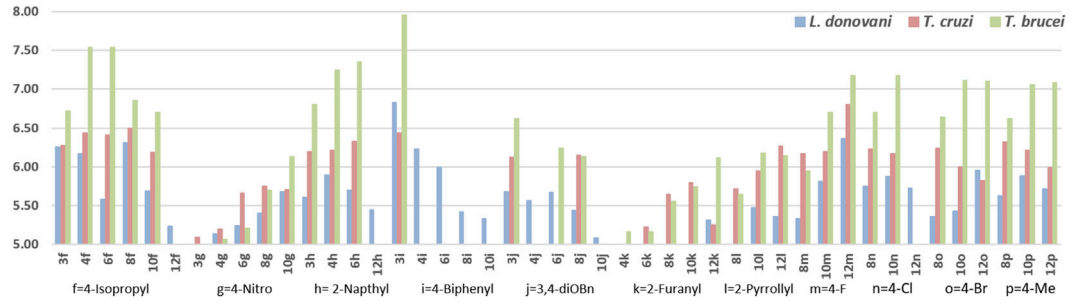

FIGURE 3
Anti-trypanosomatid activity of the analogs with pIC_{50} > 5.0.

with only compounds 4f, 6f, 8f, 3i, 8n and 10n exhibiting cytotoxicity at concentrations below 4.76 μg mL^{-1}, the highest concentration tested (Recio-Balsells et al., 2025). The biological evaluation revealed clear differences in potency among the different substitution patterns and linker lengths, enabling a detailed structure–activity relationship analysis.

Table 1; Figure 2 summarize the *in vitro* antiparasitic activity of the second-generation library against trypanosomatid species and cytotoxicity values, with several compounds exhibiting pIC_{50} values above 6.0 against one or more of the trypanosomatid species evaluated. The selectivity index (SI) was calculated as the ratio of the IC_{50} for mammalian cytotoxicity to the IC_{50} for antiparasitic activity.

Within the new collection, forty-five compounds exhibited pIC_{50} values above 5.0 against at least one of the parasites evaluated (Figure 3). Of the 4-isopropyl series (f) three of the six analogues exhibited a potent activity (pIC_{50} values >6.0) against the three trypanosomatid species. Analysis of the 4-nitro series (g) revealed that only one (10g) displayed activity against all the trypanosomatids tested (pIC_{50} values > 5.5). Among the eighteen bulkier derivatives (series h, i, j), solubility issues were encountered in the *T. cruzi* and *T. brucei* assays. Nevertheless, 5 of these analogs displayed pIC_{50} values >5.5, with 3i being the most active compound of the library against *T. brucei* (pIC_{50} = 7.96). It should be noted that the interpretation of the SAR within these bulkier aromatic series is limited by the solubility issues observed for several analogues. Consequently, the apparent activity trends should be interpreted with caution, as differences in aqueous solubility may have contributed to the observed biological profiles. Regarding the heterocyclic derivatives (k, l), their activity was notably underwhelming. Within this category, only one furan (12k) and two pyrrole (10l, 12l) analogs displayed pIC_{50} values >6.0 for *T. cruzi* and/or *T. brucei*. The focused long-chain halogenated and methyl series (m, n, o and p), proved particularly successful being active against the three trypanosomatid species evaluated. Among these analogs, 12m displayed the highest activity against *T. cruzi* and *L. donovani*. Against *T. brucei*, compounds 12m and 10n were the most active members of the series.

The influence of the diamine linker length on antitrypanosomatid activity appears to be a key determinant of biological activity. Among the evaluated series, the 4-isopropyl (f), naphthyl (h), and biphenyl (i) derivatives included some of the most potent compounds, which generally contained diamine linkers of six carbon atoms or fewer. However, interpretation of the SAR within the bulkier aromatic series should be made with caution because several analogues were affected by solubility limitations, particularly as the diamine linker length increased. In contrast, long-chain diamine analogues of the para-halogenated and para-methyl-substituted series (m, n, o, p) exhibited potent antitrypanosomatid activity without any apparent solubility issues. As for the heterocyclic series (k, l), derivatives containing diamine chains of 8 carbons or more displayed highest anti-trypanosomatid activities.

In a more detailed analysis, all isopropyl derivatives (except for 12f) yielded pIC_{50} values > 6.00 against *T. brucei* and *T. cruzi* (Figure 3). Particularly, 4f and 6f displayed significantly higher activity against *T. brucei* compared to the other analogs of the series with both compound´s exhibiting pIC_{50} values of 7.54. Regarding *L. donovani*, only 3 derivatives generated pIC_{50} values >6.00. Concerning cytotoxicity, all derivatives presented SI > 15 for *T. brucei* and *T. cruzi*, while for *L. donovani*, only 3f and 4f achieve this SI threshold.

The bulkier aromatic series also included several compounds with pIC_{50} values above 6.0, predominantly among analogues containing diamine linkers of six carbon atoms or fewer. Within the naphthyl series, compounds 4h and 6h displayed potent activity against *T. brucei* (pIC_{50} = 7.22 and 7.30, respectively) and also showed high activity against *T. cruzi* (pIC_{50} = 5.89 and 6.33).

For the biphenyl series, all compounds except 3i displayed solubility issues in the *T. cruzi* and *T. brucei* assays, limiting the interpretation of SAR within this series. Compound 3i exhibited the highest activity in the library against *T. brucei* (pIC_{50} = 7.96), *T. cruzi* (pIC_{50} = 6.43), and *L. donovani* (pIC_{50} = 6.82). However, this finding should not be overinterpreted as representative of the biphenyl series, since the remaining analogues were affected by solubility limitations that precluded a comprehensive SAR analysis. The 3,4-diOBn series (j) also displayed antitrypanosomatid activity, with the highest potency observed against *T. cruzi* and *T. brucei*. Within this series, compounds 3j, 4j, and 8j were the only analogues that did not present solubility issues in the *T. cruzi* and *T. brucei* assays. These compounds also exhibited pIC_{50} values above 6.0, except for 8j against *T. cruzi*.

As previously mentioned, the 4-nitro series (g) exhibited limited activity against trypanosomatids. Among these analogues, only compound 10g reached a pIC_{50} value above 6.00, specifically against *T. brucei* (pIC_5 = 6.13). Nevertheless, the remaining

analogues displayed moderate activity against *T. cruzi*, *T. brucei*, and *L. donovani*, with pIC_{50} values ranging from 4.70 to 5.75, except for compounds 3g and 12g. Within the nitro series, activity generally increased with linker length, reaching its maximum with the C10 analogue.

Most heterocyclic derivatives displayed relatively poor antitrypanosomatid activity; however, potency generally increased with increasing diamine linker length. Among the furan derivatives, 12k showed the highest activity against *L. donovani* and *T. brucei* with pIC_{50} values of 5.32 and 6.11, respectively. Against *T. cruzi*, 10k was the most active analogue (pIC_{50} = 5.80). Among the pyrrole derivatives, compounds 12l and 10l displayed the highest activity against *T. brucei*, with pIC_{50} values of 6.17 and 6.14, respectively. In addition, 12l also displayed potent activity against *T. cruzi* (pIC_{50} = 6.27).

The focused long-chain para-halogenated (m–o) and para-methyl-substituted (p) series displayed consistently high antitrypanosomatid activity, with pIC_{50} values ranging from 5.33 to 7.17. Among these analogs, ten exhibited pIC_{50} values above 6.0 against *T. brucei*, nine against *T. cruzi*, and one against *L. donovani*. Within the synthesized para-fluoro series (C8–C12), activity increased consistently with increasing diamine chain length, with compound 12m emerging as the most potent analogue, displaying pIC_{50} values of 6.36, 6.80, and 7.17 against *L. donovani*, *T. cruzi*, and *T. brucei*, respectively. In contrast, no consistent chain length-dependent trend was observed within the synthesized C8–C12 analogues of the para-chloro (n), para-bromo (o), or para-methyl (p) series.

Collectively, these results revealed distinct structure–activity relationship patterns across the different aromatic series, highlighting the influence of both aromatic substitution and diamine linker length on antitrypanosomatid potency. Overall, the diamine analogues displayed the highest activity against *T. brucei*, followed by *T. cruzi* and, to a lesser extent, *L. donovani*. Among the compounds tested, 16 exhibited superior potency against *T. brucei* relative to the reference drug nifurtimox (pIC_{50} = 5.77), while 17 outperformed nifurtimox against *T. cruzi* (pIC_{50} = 5.68). In the case of *L. donovani*, only compound 3i displayed greater activity than amphotericin B (pIC_{50} = 6.49), although 57% of the library exhibited higher activity than pentamidine (pIC_{50} = 5.21).

2.2.2 Potency of selected hits against promastigote and amastigote of *Leishmania* spp. and cytotoxicity assays in BMDMs

To further explore the antileishmanial potential of this scaffold, nine representative derivatives from the first- and second-generation N,N′-disubstituted aliphatic diamine libraries were advanced for expanded biological evaluation. The selected compounds captured the most promising activity profiles while preserving the structural diversity identified during the SAR analysis, and were chosen based on antiparasitic potency, selectivity indices, and chemical diversity. From the first-generation library, the a 4-benzyloxy derivative 4c, the most active compound against *L. donovani* promastigote, with a pIC_{50} of 7.51 and broad trypanosomatid activity. Compound 8c was additionally selected to evaluate the influence of a longer diamine linker while maintaining good antiparasitic activity. The 3-methoxy-4-benzyloxy series (e) also emerged as a promising chemotype, displaying pIC_{50} values above 6.0 against *L. donovani* promastigotes as well as the other trypanosomatids evaluated. Because biological activity was comparable among analogues bearing diamine linkers from C3 to C8, compounds 4e and 8e were selected to enable direct comparison with the corresponding 4-benzyloxy derivatives (4c and 8c). Finally, compounds 12a, 12m, and 10g were selected as representative long-chain analogues combining high antiparasitic potency, excellent selectivity indices, and structurally simple aromatic substitution patterns.

To determine the broader therapeutic potential of this scaffold, we expanded our evaluation to include both the promastigote and the clinically relevant intracellular amastigote stage across a panel of *Leishmania* spp., including *L. amazonensis*, *L. braziliensis*, and *L. infantum*. These experiments assessed intracellular activity in a macrophage infection model across multiple *Leishmania* species, providing an initial indication of the scaffold's potential to target parasites associated with both cutaneous and visceral leishmaniasis. Biological evaluation of the selected hits is summarized in Table 2; Figure 4. Overall, the selected hits displayed higher activity against the amastigote stage compared to the promastigote stage. Notably, all compounds exhibited pIC_{50} values above 6.00 against the amastigote stage across the three *Leishmania* spp. tested, except for compounds 4e and 10g against *L. braziliensis*. Moreover, several compounds, 8e, 12m, 10g, and 6i, displayed pIC_{50} values above 7.0 against two species. Interestingly, the nitro-analog 10g exhibited pIC_{50} values of 7.40 and 7.10 against the amastigote stage of *L. amazonensis* and *L. infantum*, respectively, but showed a substantial decrease in activity (pIC_{50} < 5.40) against *L. braziliensis*. This species-dependent difference may reflect variations in nitroreductase expression or activity, or other intrinsic determinants of nitro-compound susceptibility. However, this hypothesis remains speculative and will require dedicated mechanistic studies to establish its biological basis. Distinct profiles in drug sensitivity among *Leishmania* species are a recognized phenomenon across multiple antileishmanial agents (Zauli-Nascimento et al., 2010; Coser et al., 2021). In contrast, against the promastigote stage, only four hits showed pIC_{50} values above 6.0 for *L. amazonensis* and *L. infantum*, and five for *L. braziliensis*. Overall, these results demonstrate that the selected diamine analogues retain high levels of activity against the clinically relevant intracellular amastigote stage across multiple *Leishmania* species, despite the generally lower potency observed against promastigotes.

Among the selected 4-OBn derivatives, compound 4c exhibited comparable activity against the three *Leishmania* species at both parasite stages, with pIC_{50} values ranging from 6.20 to 6.77. In contrast, compound 8c displayed a clear preference for the amastigote stage, exhibiting slightly higher activity than 4c. Within the 3-OMe,4-OBn series, compound 8e displayed the highest activity among the selected hits against the amastigote stage of *L. amazonensis* and *L. braziliensis*, with pIC_{50} values of 7.70 and 7.46, respectively. Compared with 8c, this increase in activity suggests a favorable contribution of the 3-OMe substituent to antileishmanial activity. Nonetheless, 8e was less active against *L. infantum* amastigotes, although it still maintained a pIC_{50} value of 6.43. Compound 4e showed activity comparable to that of 4c, except for a pronounced decrease in activity against *L. braziliensis* amastigotes.

Among the long-chain analogues, compounds 12a and 12m displayed broadly comparable activity profiles, although the para-

10.3389/fchbi.2026.1888764

TABLE 2 Biological evaluation of selected hits against a panel of *Leishmania* spp. Endemic in South America.

Id	n	R	*L.* Amazonensis		*L. braziliensis*		*L. infantum*	
			(p)	(a)	(p)	(a)	(p)	(a)
4c	4	4-OBn	6.74	6.77	6.28	6.66	6.44	6.59
8c	8	4-OBn	5.73	6.80	5.39	6.70	5.63	6.85
4e	4	3-OMe,4-OBn	6.47	6.85	6.21	5.84	6.22	6.89
8e	8	3-OMe,4-OBn	5.72	7.70	6.27	7.46	6.25	6.43
12a	12	H	5.72	6.82	5.50	7.00	5.61	6.82
12m	12	F	6.24	6.92	6.06	7.00	5.65	7.40
10g	10	NO_2	5.50	7.40	5.39	<5.40	5.51	7.10
6i	6	Biphenyl	5.82	7.15	5.73	6.74	5.72	7.00
4h	4	Naphtyl	6.12	7.52	6.02	6.89	5.58	6.77
Miltefosine			4.77	5.71	4.46	5.55	4.75	5.89

Legend: (p), promastigotes; (a), amastigotes.

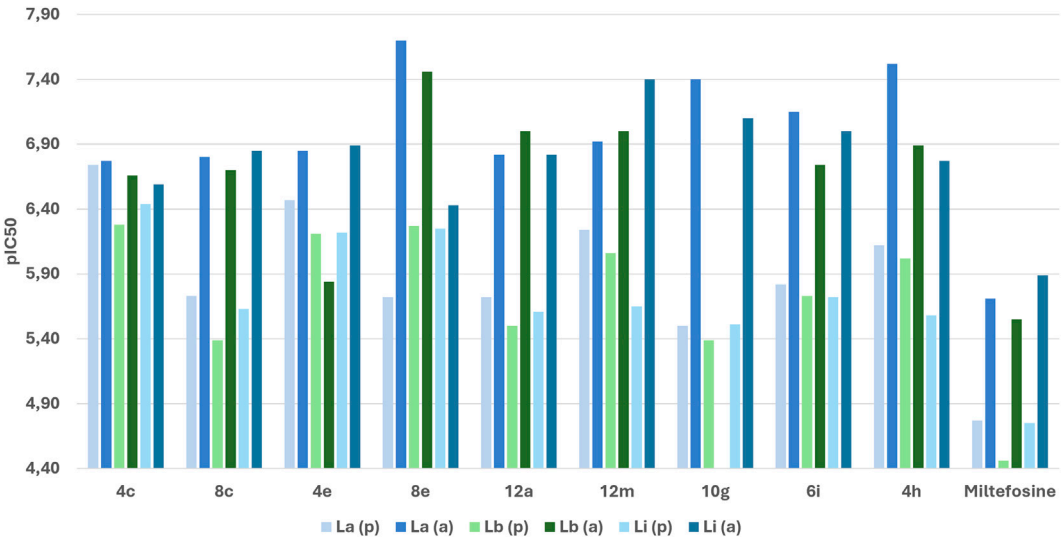

FIGURE 4
Selective hits activity against *Leishmania* spp. La(p): *L. amazonensis* promastigotes, La(a): *L. amazonensis* amastigotes, Lb(p): *L. braziliensis* promastigotes, Lb(a): *L. braziliensis amastigotes*, Li(p): *L. infantum* promastigotes, Li(a): *L. infantum* amastigotes.

fluoro derivative 12m consistently exhibited higher potency. In particular, 12m displayed the highest activity against *L. infantum* amastigotes with a pIC_{50} of 7.40, as well as strong activity against *L. braziliensis* and *L. amazonensis* amastigotes, with pIC_{50} values of 7.00 and 6.92, respectively. The nitro derivative 10g exhibited outstanding activity against *L. amazonensis* and *L. infantum* amastigotes, but markedly lower activity against *L. braziliensis*.

The bulky aromatic derivatives 6i and 4h also displayed comparable activity profiles. Compound 4h was more active against *L. amazonensis* and *L. braziliensis*, whereas 6i exhibited higher potency against *L. infantum*.

Although these results demonstrate potent activity against intracellular amastigotes, it should be noted that, as with any intracellular infection model, these assays do not exclude a contribution of host cell-mediated parasite killing. Therefore, additional mechanistic studies will be required to distinguish direct antiparasitic activity from host-mediated effects.

Finally, to further assess compound selectivity under physiologically relevant conditions, the selected hit compounds were evaluated for cytotoxicity against BMDMs, the same host cells used in the intracellular amastigote assays. The selectivity index (SI) based on BMDMs was considered the primary selectivity metric for intracellular assays, whereas the SI determined in Vero cells was used as supportive information. Cytotoxicity data obtained in BMDMs, together with the previously determined values in Vero cells and the corresponding

TABLE 3 Selectivity index of the selected hits against *Leishmania* spp.

Compound	BMDMs pEC_{50}	Vero cells pEC_{50}	SI *La (a)* BMDM	SI *Lb (a)* BMDM	SI *Li (a)* BMDM	SI *La (a)* vero	SI *Lb (a)* vero	SI *Li (a)* vero
4c	6.10	5.23	4.7	3.6	3.07	34.3	26.5	22.4
8c	5.52	<5.05	18.8	15.1	21.5	>55.4	>44.4	>63.4
4e	5.97	<5.06	7.6	0.7	8.15	>62.9	>6.1	>67.7
8e	5.98	5.34	52.5	30.0	2.83	226.0	129.1	12.2
12a	5.67	<4.90	14.4	21.6	14.4	>83.3	>125.0	>83.3
12m	5.64	<4.94	18.9	22.7	56.8	>95.0	>114.0	>285.0
10g	5.75	<4.97	44.0	-	22.0	>270.0	-	>135.0
6i	5.76	<4.97	24.6	9.6	17.6	>151.4	>58.9	>106.0
4h	6.25	<4.89	18.6	4.3	0.43	>430.0	>99.2	>75.9
Miltefosine	4.33	-	24.0	16.6	35.9	-	-	-

La (a): L. amazonensis amastigotes. *Lb (a): L. braziliensis* amastigotes. *Li (a): L. infantum* amastigotes. SI: Selectivity index. EC_{50} (BMDMs, or Vero cells)/IC_{50} (amastigote). Red: SI < 1; Yellow 1≤IS < 10; Green ≥10.

TABLE 4 Physicochemical parameters estimations of the selected hits.

Compound	Lipinski	Water sol. (μM)[#]	SI *La (a)* BMDM	SI *Lb (a)* BMDM	SI *Li (a)* BMDM	SI ≥ 10
4c	✓	0.79 (PS)	4.7	3.6	3.07	✗
8c	✗	0.05 (PS)	18.8	15.1	21.5	✓
4e	✓	0.06 (PS)	7.6	0.7	8.15	✗
8e	✗	0.004 (PS)	52.5	30.0	2.83	✗
12a	✓	1.50 (MS)	14.4	21.6	14.4	✓
12m	✓	0.71 (PS)	18.9	22.7	56.8	✓
10g	✓	5.33 (MS)	44.0	-	22.0	✗
6i	✓	0.19 (PS)	24.6	9.6	17.6	✗
4h	✓	2.70 (MS)	18.6	4.3	0.43	✗

Water sol. (μM)[#]: ESOL water solubility estimation (Swiss ADME).
The LogS scale is defined as: insoluble (< −10), poorly soluble (−10 to −6), moderately soluble (−6 to −4), soluble (−4 to −2), very soluble (−2 to 0), and highly soluble (>0). MS: moderately soluble, PS: poorly soluble. **SI**: selective index.
La: L. amazonensis. *Lb*: L. braziliensis. *Li*: L. infantum.

SI values, are summarized in Table 3. The SI values reported in Table 1 were derived from Vero cells using a maximum tested concentration of 4.76 μg mL^{-1} and should therefore be interpreted as lower bounds when the CC_{50} was not reached. All compounds displayed measurable cytotoxicity against BMDMs, with pEC_{50} values ranging from 5.52 to 6.25. Nevertheless, compounds 8c, 12a, and 12m exhibited SI values above 10 against the amastigote stage of the three species when compared with BMDMs. Regarding selectivity relative to Vero cells, all compounds showed SI values above 10, except for 10g and 4e against *L. braziliensis*, which is consistent with their lower antiparasitic activity against this species. The higher cytotoxicity observed in BMDMs compared with Vero cells may reflect intrinsic biological differences between primary macrophages and immortalized epithelial cells. Macrophages display high constitutive endocytic and phagocytic activity, which may increase intracellular exposure to the compounds, whereas Vero cells exhibit distinct physiological and uptake characteristics. Similar differences between primary cells and immortalized cell lines have been widely reported in antiparasitic drug discovery (Horvath et al., 2016). Accordingly, for intracellular infection assays, the selectivity indices calculated using BMDMs provide a more physiologically relevant assessment of compound selectivity than those obtained using Vero cells.

The physicochemical properties of the second-generation library were previously estimated (Recio-Balsells et al., 2025). Table 4 summarizes the relevant physicochemical parameters of the selected hit compounds, as calculated using the SwissADME platform (Daina et al., 2017). Given the potent activity of nearly all selected compounds against the intracellular amastigote stage of the three *Leishmania* species, the selectivity indices together with the

predicted physicochemical properties were used to prioritize the most promising hit compounds.

Among the compounds exhibiting the highest selectivity índices (8c, 12a and 12m) the benzyl-unsubstituted analog 12a showed the most favorable profile, complying with the Lipinski rule and displaying an estimated moderate aqueous solubility. Compound 12m also complied with these criteria, although it was predicted to be poorly soluble. In contrast, 8c did not comply with Lipinski's rule and was also predicted to have poor aqueous solubility. Importantly, it is important to note that for cutaneous leishmaniasis, topical administration could be considered as an alternative to oral delivery. Furthermore, the structure–activity relationship findings obtained in this study provide a valuable basis for a new round of scaffold optimization aimed at improving aqueous solubility while maintaining antileishmanial activity and selectivity.

Overall, compound 12a emerged as the most balanced hit, combining broad-spectrum antileishmanial activity, favorable selectivity indices, compliance with Lipinski's rule, and the most favorable predicted physicochemical profile among the compounds evaluated. Nevertheless, compound 12m also represents an attractive lead, as it combined excellent antileishmanial potency and selectivity with a para-fluoro substitution that may confer improved metabolic stability, making it an appealing candidate for further biological evaluation. Accordingly, future optimization efforts will focus on reducing lipophilicity while preserving antileishmanial potency and selectivity through rational structural modifications, including the incorporation of additional polar functional groups and/or a reduction in the aromatic content of the scaffold.

3 Conclusions

In summary, the second-generation N,N′-disubstituted diamine library was evaluated against the extracellular stages of *L. donovani*, *T. brucei*, and *T. cruzi*. The screening identified several highly potent antitrypanosomatid analogues and established distinct structure–activity relationship (SAR) trends across the different aromatic series. Among the parasites evaluated, *T. brucei* was the most susceptible species, followed by *T. cruzi*, whereas *L. donovani* displayed comparatively lower sensitivity.

The newly synthesized compounds expanded the structure–activity relationship (SAR) landscape of this scaffold, revealing a clear interplay between diamine linker length and the structural characteristics of the terminal aromatic substituent. In general, several bulkier aromatic substituents favored activity in analogues bearing short diamine linkers, whereas longer linkers (particularly C10 and C12) were generally associated with improved activity in unsubstituted benzyl, para-halogenated, nitro, and heteroaromatic derivatives.

To further advance this scaffold within the antileishmanial drug discovery pipeline, nine representative compounds were selected for expanded evaluation against *L. amazonensis*, *L. braziliensis*, and *L. infantum* in both promastigote and intracellular amastigote stages. Several analogues displayed pIC_{50} values above 6.0 across all three species, with generally higher potency against the clinically relevant intracellular amastigote stage. Cytotoxicity assays performed in BMDMs, the corresponding host cells, identified compounds 8c, 12a, and 12m as the most selective members of the series, each exhibiting selectivity indices above 10.

Overall, these findings demonstrate the broad antitrypanosomatid, and particularly antileishmanial, potential of this diamine scaffold. Compound 12a emerged as the most balanced lead, combining broad-spectrum activity, favorable selectivity, and predicted drug-like properties, whereas compound 12m represents an attractive complementary lead owing to its excellent antileishmanial potency and the potential pharmacokinetic advantages associated with para-fluorine substitution. Together with compound 8c, these analogues provide a strong foundation for further lead optimization and preclinical evaluation within the *Leishmania* drug discovery pipeline.

4 Experimental section

4.1 Biological assays against parasites

4.1.1 *In vitro* activity against *T. brucei brucei*

T. brucei (MIT at 427 strain; clone 221a) bloodstream form trypomastigotes were seeded at 1×10^3 mL^{-1} in 200 µL modified Iscove´s medium containing different concentrations of the compounds. After incubation at 37 °C under a 5% CO_2 atmosphere for 3 days, 20 µL Alamar blue (Biosource UK Ltd.) was added to each well and the plates were further incubated at 37 °C for 16 h. The fluorescence of each culture was determined using a Germini Fluorescent Plate reader (Molecular Devices) at an excitation wavelength of 530 nm, emission wavelength of 585 nm and a filter cut off at 550 nm, and the IC_{50} established. The color change resulting from the reduction of Alamar blue is proportional to the number of live cells, which was established following production of a standard curve.

4.1.2 *In vitro* activity against *T. cruzi* epimastigotes

T. cruzi (clone CL-Brener) epimastigotes were seeded at 5×10^5 mL^{-1} in 200 µL modified RPMI-1640 medium (without glutamate) (Martinez et al., 2023) containing different concentrations of diamine and 20 µL Alamar blue (Biosource UK Ltd.) was added to each well. After incubation at 27 °C for 14 days, the cell densities were determined by monitoring the fluorescence of each culture as described above and the IC_{50} value for each compound established.

4.1.3 *In vitro* activity against *L. donovani* promastigotes

Leishmania donovani promastigotes of the S1 Sudan strain (2×10^6 cell mL^{-1}) were cultured at 26 °C in plastic flasks (25 cm^2), containing RPMI-1640 medium (without sodium bicarbonate and sodium pyruvate) with 10% (v/v) fetal bovine serum. Subculture of *L. donovani* promastigotes twice a week, with highest concentration cells in the range of 20–25 × 10^6 promastigotes mL^{-1}. Antileishmanial activity of the compounds was tested *in vitro* on a culture of *L. donovani* promastigotes. In a 96-well microplate the compounds with appropriate dilution were added to the promastigotes culture (2×10^6 cell mL^{-1}) to get the final concentrations of 40, 8 and 1.6 µg mL^{-1}. The plates were incubated at 26 °C for 72 h and growth was determined using

Alamar blue assay (Mikus et al., 2000). Pentamidine and Amphotericin B were used as the standard antileishmanial and DMSO was used as negative control. IC_{50} values were obtained by non-linear regression of dose response logistic functions, using the Microsoft Excel-based plug-in XLfit. The assays were performed in triplicate.

4.1.4 *In vitro* activity against *L. amazonensis, L. braziliensis and L. infantum* promastigotes

Promastigotes of *L. amazonensis* (MHOM/BR/1973/M2269), *L. braziliensis* (MHOM/BR/94/H3227) and *L. infantum* (MHOM/BR/1972/LD) were grown at 25 °C in 199 medium (M199) (Sigma-Aldrich) supplemented with HEPES 40 mM [pH 7.4], adenine 0.1 mM, hemin 0.005%, 10% heat-inactivated fetal bovine serum and 100 μg mL^{-1} of penicillin/streptomycin (Kapler et al., 1990). For the cultivation of *L. braziliensis* and *L. infantum,* M199 was supplemented with 2% sterile human urine (Howard et al., 1991).

The susceptibility of *Leishmania* promastigotes to compounds was determined using the MTT (3-(4,5-dimethylthiazol-2-yl)-2,5-diphenyltetrazoline bromide) colorimetric assay, after incubation of 2×10^6 promastigotes per well in a 96-well plate in M199 (Sigma-Aldrich) for 24 h at 25 °C in the presence of increasing concentrations of the each compound (0, 0.07, 0.15, 0.31, 0.62, 1.25, 2.5 and 5 μM), as described previously (Caminos et al., 2012). The experiments were carried out in triplicate and at least three independent experiments were performed for each compound. The 50% effective concentration (IC_{50}) was determined by sigmoidal regression curves obtained by the GraphPad Prism 7 software.

4.1.5 *In vitro* activity against *L. amazonensis, L. braziliensis* and *L. infantum* amastigotes

To determine the susceptibility of intracellular *Leishmania* amastigotes to each compound, bone-marrow derived macrophages (BMDMs) were differentiated as previously described (Zamboni and Rabinovitch, 2003). Macrophages were plated at a density of 3×10^5 macrophages per well in complete RPMI 1640 medium in 24-well plate. Late-stage promastigotes were used to infect macrophages at a macrophage/parasite ratio of 1:5 for *L. amazonensis*, 1:20 for and 1:30 for. Four hours after infection at 5% CO_2 and temperature of 34 °C for *L. amazonensis* and *L. braziliensis,* while the temperature of 37 °C was used for *L. infantum*, non-internalized promastigotes were removed by washing with warmed PBS. Infected macrophages were maintained in RPMI 1640 medium at different concentrations of each compound (0.05, 0.1, 0.5, 1, 1.5, 2 and 4 μM) for 72 h, 5% CO_2 and the corresponding temperature depending on the *Leishmania* species. Afterwards, macrophages were fixed with methanol and stained with Giemsa. The percentage of infection and number of amastigotes per infected macrophage were determined by counting at least 100 macrophages in three independent experiments that were used to determine IC_{50} values as described above.

4.2 Cytotoxicity evaluation against BMDMs

For cytotoxicity assays, BMDMs were obtained from female 4 to 5-weeks-old BALB/c mice. Protocol and procedures involving mice for isolation of BMDMs were approved by the Ethics Committee for Animal Experimentation of the Instituto de Biologia, Universidade Estadual de Campinas (UNICAMP) (protocol no. 5719-1/2021).

Macrophages in a 500 μL suspension (3×10^5 macrophages per well) were allowed to adhere to the bottom of 24-well plate for 24 h at 37 °C. After the initial incubation, the macrophages were incubated in complete RPMI 1640 medium with increasing concentrations of each compound used (0.625, 1.25, 2.5, 5, 10 and 20 μM) for 72 h. After this period, the RPMI medium containing each compound was removed and then 100 μL of trypsin was added and incubated for 15 min. Then, 400 μL of PBS was added and 10 μL of cell suspension was added to 10 μL of 0.4% Trypan Blue (Sigma Aldrich Corp., St. Louis, MO, USA). Ten microliters of the resuspension were plated in the Neubauer chamber, followed by counting the total number of viable and non-viable macrophages. Cells that acquired the blue dye were considered non-viable. Experiments were performed in duplicate and at least three independent experiments were performed for each compound. To be considered a low toxicity compound/drug, it must be, at least, 10 times more active against the parasite than for the host cell; in other words, the selectivity index (SI) (CC_{50} for mammalian cell line/EC_{50} of the parasite) must be ≥10 (Ioset et al., 2009).

Data availability statement

The raw data supporting the conclusions of this article will be made available by the authors, without undue reservation.

Ethics statement

Protocol and procedures involving mice for isolation of BMDMs were approved by the Ethics Committee for Animal Experimentation of the Instituto de Biologia, Universidade Estadual de Campinas (UNICAMP) (protocol no. 5719-1/2021).

Author contributions

AR-B: Data curation, Writing – original draft, Investigation, Formal Analysis, Writing – review and editing. EP-Z: Investigation, Writing – review and editing, Data curation, Formal Analysis. EC: Data curation, Methodology, Investigation, Writing – review and editing, Formal Analysis. BF: Writing – review and editing, Formal Analysis, Methodology, Investigation, Data curation. AC: Methodology, Writing – review and editing, Conceptualization, Data curation, Investigation, Formal Analysis, Funding acquisition, Resources, Project administration. SW: Resources, Funding acquisition, Formal Analysis, Writing – review and editing, Data curation, Conceptualization, Project administration, Investigation, Methodology. BT: Conceptualization, Investigation, Data curation, Writing – review and editing, Methodology, Resources, Funding acquisition, Formal Analysis, Project administration. GL: Funding acquisition, Resources, Formal Analysis, Project administration, Supervision, Data curation, Writing – review and editing, Methodology, Conceptualization, Writing – original draft.

Funding

The author(s) declared that financial support was received for this work and/or its publication. This work was supported in part by grants from the National Research Council of Argentina, CONICET (PIP 2021-2023 11220200101045CO to G.R.L.); Agencia Nacional de Promoción Científica y Tecnológica, ANPCyT-Argentina (ANPCyT PICT 2021-I-A-00512 awarded to G.R.L.); UNR (Universidad Nacional de Rosario 80020190300101UR); Fundação de Amparo à Pesquisa do Estado de São Paulo (FAPESP) (grant number 2016/21171-6) and the Conselho Nacional de Desenvolvimento Científico e Tecnológico (CNPq) (grant number 405235/2021-6). The research leading to these results has, in part, received funding from the UK Research and Innovation via the Global Challenges Research Fund under grant agreement A Global Network for Neglected Tropical Diseases grant number MR/P027989/1. G.R.L. is a member of the scientific staff of CONICET.

Conflict of interest

The author(s) declared that this work was conducted in the absence of any commercial or financial relationships that could be construed as a potential conflict of interest.

The author GL declared that they were an editorial board member of Frontiers at the time of submission. This had no impact on the peer review process and the final decision.

Generative AI statement

The author(s) declared that generative AI was used in the creation of this manuscript. Artificial intelligence (ChatGPT, OpenAI) was used solely to improve English grammar, spelling, and readability.

Any alternative text (alt text) provided alongside figures in this article has been generated by Frontiers with the support of artificial intelligence and reasonable efforts have been made to ensure accuracy, including review by the authors wherever possible. If you identify any issues, please contact us.

Publisher's note

Supplementary material

The Supplementary Material for this article can be found online at: https://www.frontiersin.org/articles/10.3389/fchbi.2026.1888764/full#supplementary-material

References

Bacchi, C. J., Nathan, H. C., Hutner, S. H., McCann, P. P., and Sjoerdsma, A. (1980). Polyamine metabolism: a potential therapeutic target in trypanosomes. *Science* 210 (4467), 332–334. doi: 10.1126/science.6775372

Braillard, S., Keenan, M., Breese, K. J., Heppell, J., Abbott, M., Islam, R., et al. (2023). DNDI-6174 is a preclinical candidate for visceral leishmaniasis that targets the cytochrome bc1. *Sci. Transl. Med.* 15 (726), eadh9902. doi: 10.1126/scitranslmed.adh9902

Caminos, A. P., Panozzo-Zenere, E. A., Wilkinson, S. R., Tekwani, B. L., and Labadie, G. R. (2012). Synthesis and antikinetoplastid activity of a series of N,N′-Substituted diamines. *Bioorg. Med. Chem. Lett.* 22 (4), 1712–1715. doi: 10.1016/j.bmcl.2011.12.101

Coser, E. M., Ferreira, B. A., Yamashiro-Kanashiro, E. H., Lindoso, J. A. L., and Coelho, A. C. (2021). Susceptibility to paromomycin in clinical isolates and reference strains of leishmania species responsible for tegumentary leishmaniasis in Brazil. *Acta Trop.* 215, 105806. doi: 10.1016/j.actatropica.2020.105806

Daina, A., Michielin, O., and Zoete, V. (2017). SwissADME: a free web tool to evaluate pharmacokinetics, drug-likeness and medicinal chemistry friendliness of small molecules. *Sci. Rep.* 7 (1), 42717. doi: 10.1038/srep42717

DNDi (2026). *Drugs for Neglected Diseases Initiative (DNDi)*. Available online at: https://dndi.org/research-development/portfolio/dndi-6148-chagas/(Accessed: May 2026).

Fairlamb, A. H., Blackburn, P., Ulrich, P., Chait, B. T., and Cerami, A. (1985). Trypanothione: a novel bis(glutathionyl)spermidine cofactor for glutathione reductase in trypanosomatids. *Science* 227 (4693), 1485–1487. doi: 10.1126/science.3883489

Horvath, P., Aulner, N., Bickle, M., Davies, A. M., Del Nery, E., Ebner, D., et al. (2016). Screening out irrelevant cell-based models of disease. *Nat. Rev. Drug Discov.* 15, 751–769. doi: 10.1038/nrd.2016.175

Howard, M. K., Pharoah, M. M., Ashall, F., and Miles, M. A. (1991). Human urine stimulates growth of leishmania *in vitro*. Trans. *R. Soc. Trop. Med. Hyg.* 85 (4), 477–479. doi: 10.1016/0035-9203(91)90226-O

Ioset, J. R., Brun, R., Wenzler, T., Kaiser, M., and Yardley, V. (2009). "Drug screening for kinetoplastids diseases," in *A Training Manual for Screening in Neglected Diseases*.

Kapler, G. M., Coburn, C. M., and Beverley, S. M. (1990). Stable transfection of the human parasite Leishmania major delineates a 30-Kilobase region sufficient for extrachromosomal replication and expression. *Mol. Cell. Biol.* 10 (3), 1084–1094. doi: 10.1128/mcb.10.3.1084-1094.1990

Ma, Z., Augustijn, K., De Esch, I., and Bossink, B. (2023). Public-private partnerships influencing the initiation and duration of clinical trials for neglected tropical diseases. *PLoS Negl. Trop. Dis.* 17 (11), 1–14. doi: 10.1371/journal.pntd.0011760

Martín-Montes, Á., Clares, M. P., Martín-Escolano, R., Delgado-Pinar, E., Marín, C., Verdejo, B., et al. (2021). Heterocyclic diamines with leishmanicidal activity. *ACS Infect. Dis.* 7 (12), 3168–3181. doi: 10.1021/acsinfecdis.1c00215

Martinez, M. Z., Olmo, F., Taylor, M. C., Caudron, F., and Wilkinson, S. R. (2023). Dissecting the interstrand crosslink DNA repair system of Trypanosoma cruzi. *DNA Repair* 125, 103485. doi: 10.1016/j.dnarep.2023.103485

Mikus, J., and Steverding, D. (2000). A simple colorimetric method to screen drug cytotoxicity against leishmania using the dye alamar blue®. *Parasitol. Int.* 48 (3), 265–269. doi: 10.1016/S1383-5769(99)00020-3

Mollo, M. C., Cambiaso, M. L., Ferreira, L. L. G., Kilimciler, N. B., Bisceglia, J. A., Andricopulo, A. D., et al. (2025). Synthesis and *in vitro* leishmanicidal activity of novel N-arylspermidine derivatives. *Bioorg. Chem.* 154, 108083. doi: 10.1016/j.bioorg.2024.108083

Mowbray, C. E., Braillard, S., Glossop, P. A., Whitlock, G. A., Jacobs, R. T., Speake, J., et al. (2021). DNDI-6148: a novel benzoxaborole preclinical candidate for the treatment of visceral leishmaniasis. *J. Med. Chem.* 64 (21), 16159–16176. doi: 10.1021/acs.jmedchem.1c01437

Mukhopadhyay, R., and Madhubala, R. (1995). Effects of bis(benzyl)polyamine analogs on Leishmania donovani promastigotes. *Exp. Parasitol.* 81 (1), 39–46. doi: 10.1006/expr.1995.1090

Nagle, A., Biggart, A., Be, C., Srinivas, H., Hein, A., Caridha, D., et al. (2020). Discovery and characterization of clinical candidate LXE408 as a kinetoplastid-selective proteasome inhibitor for the treatment of leishmaniases. *J. Med. Chem.* 63 (19), 10773–10781. doi: 10.1021/acs.jmedchem.0c00499

Olías-Molero, A. I., de la Fuente, C., Cuquerella, M., Torrado, J. J., and Alunda, J. M. (2021). Antileishmanial drug discovery and development: time to reset the model? *Microorganisms* 9 (12), 2500. doi: 10.3390/microorganisms9122500

Pathak, S., Bhardwaj, M., Agrawal, N., and Bhardwaj, A. (2023). A comprehensive review on potential candidates for the treatment of chagas disease. *Chem. Biol. Drug Des.* 102 (3), 587–605. doi: 10.1111/cbdd.14257

Phillips, M. A. (2018). Polyamines in protozoan pathogens. *J. Biol. Chem.* 293 (48), 18746–18756. doi: 10.1074/jbc.TM118.003342

Rao, S. P. S., Barrett, M. P., Dranoff, G., Faraday, C. J., Gimpelewicz, C. R., Hailu, A., et al. (2019). Drug discovery for kinetoplastid diseases: future directions. *ACS Infect. Dis.* 5 (2), 152–157. doi: 10.1021/acsinfecdis.8b00298

Recio-Balsells, A. I., Panozzo-Zénere, E., Carlucci, R., Chaurasia, N., Manhas, A., Fioressi, M. B., et al. (2025). Advancing N,N′-Disubstituted diamines in antimalarial drug development: structure-Activity relationships and mechanistic studies. *Eur. J. Med. Chem.* 291, 117630. doi: 10.1016/j.ejmech.2025.117630

Recio-Balsells, A. I., Reigada, C., Mediavilla, M. G., Panozzo-Zénere, E., Villarreal Parra, M., Doyle, P. S., et al. (2026). Mechanistic exploration of N,N′-Disubstituted diamines as promising chagas disease treatments. *Pharmaceuticals* 19 (1), 119. doi: 10.3390/ph19010119

Selvapandiyan, A., Shital, S., Sangma, D. A., Jain, M., Karunaweera, N., and Ganguly, N. K. (2025). An update on clinical and pathogenic spectra of leishmaniasis. *Expert Rev. Mol. Med.* 27, e27. doi: 10.1017/erm.2025.4

Singh, S., Mukherjee, A., Khomutov, A. R., Persson, L., Heby, O., Chatterjee, M., et al. (2007). Antileishmanial effect of 3-Aminooxy-1-Aminopropane is due to polyamine depletion. *Antimicrob. Agents Chemother.* 51 (2), 528–534. doi: 10.1128/aac.01055-06

Singh, S., Jhingran, A., Sharma, A., Simonian, A. R., Soininen, P., Vepsalainen, J., et al. (2008). Novel agmatine analogue, γ-guanidinooxypropylamine (GAPA) efficiently inhibits proliferation of Leishmania donovani by depletion of intracellular polyamine levels. *Biochem. Biophys. Res. Commun.* 375 (1), 168–172. doi: 10.1016/j.bbrc.2008.07.143

Thomas, M. G., De Rycker, M., Ajakane, M., Albrecht, S., Álvarez-Pedraglio, A. I., Boesche, M., et al. (2019). Identification of GSK3186899/DDD853651 as a preclinical development candidate for the treatment of visceral leishmaniasis. *J. Med. Chem.* 62 (3), 1180–1202. doi: 10.1021/acs.jmedchem.8b01218

World Health Organization (WHO) (2021). *Ending the Neglect to Attain the Sdgs: A Roadmap for Neglected Tropical Diseases 2021–2030*. Geneva: WHO.

World Health Organization (WHO). (2026a). Available online at: https://www.who.int/news-room/fact-sheets/detail/leishmaniasis (Accessed: May 2026).

World Health Organization (WHO). (2026b). Available online at: https://www.who.int/news-room/fact-sheets/detail/chagas-disease-(american-trypanosomiasis (Accessed May, 2026).

World Health Organization (WHO). (2026c). Available online at: https://www.who.int/news-room/fact-sheets/detail/trypanosomiasis-human-african-(sleeping-sickness (Accessed May, 2026).

Wyllie, S., Roberts, A. J., Norval, S., Patterson, S., Foth, B. J., Berriman, M., et al. (2016). Activation of bicyclic nitro-Drugs by a novel nitroreductase (NTR2) in leishmania. *PLoS Pathog.* 12 (11), 1–22. doi: 10.1371/journal.ppat.1005971

Zamboni, D. S., and Rabinovitch, M. (2003). Nitric oxide partially controls Coxiella burnetii phase II infection in mouse primary macrophages. *Infect. Immun.* 71 (3), 1225–1233. doi: 10.1128/iai.71.3.1225-1233.2003

Zauli-Nascimento, R. C., Miguel, D. C., Yokoyama-Yasunaka, J. K. U., Pereira, L. I. A., Pelli de Oliveira, M. A., Ribeiro-Dias, F., et al. (2010). *In vitro* sensitivity of leishmania (viannia) braziliensis and leishmania (leishmania) amazonensis Brazilian isolates to meglumine antimoniate and amphotericin B. *Trop. Med. Int. Health.* 15 (1), 68–76. doi: 10.1111/j.1365-3156.2009.02414.x